Microdisk and Microring lasers of Thiophene-Phenylene Co-oligomers embedded in SiO_2 substrates

F. Sasaki, S. Kobayashi,

Photonics Research Institute, National Institure of Advanced Industrial Science and Technology(AIST), Tsukuba, Ibaraki 305-8568, Japan.

S. Haraichi

Nanoelectronics Research Institute, AIST, Tsukuba, Ibaraki 305-8568, Japan.

S. Fujiwara, K. Bando, Y. Masumoto

Institute of Physics and Tsukuba Advanced Research Alliance (TARA), University of Tsukuba, Tsukuba, 305-8571, Japan

S. Hotta

Department of Macromolecular Science and Engineering, Graduate School of Science and Technology, Kyoto Institute of Technology, Kyoto 606-8585, Japan

Abstract

Microdisk and microring lasers of the organic semiconductor material thiophene/phenylene co-oligomer (TPCO) have been fabricated on Si/SiO_2 substrates. Laser emission with the whispering gallery modes (WGM) is observed in 0-1 vibration transitions. Comparing with the bulk film parts, a few times reduction of the lasing threshold has been observed in microdisks. Microring lasing threshold is reduced further when the width of the waveguide is less than 1 μm. WGM with waveguide confinement is supposed to contribute to the decrease of the threshold.

Thiophene/phenylene co-oligomers (TPCO) are attracting much attention as potentially useful materials for photonic devices[1-15]. The TPCO crystals show the good performance of field effect transistors[3,4] and electroluminescence[5,6] and show the high photo-excited emission yields even at room temperature. Crystals of TPCO also exhibit amplified spontaneous emission (ASE) under a high intensity excitation at room temperature[7,8]. Laser oscillation has been demonstrated as well[9,10]. Both the good performance of electronic and photonic properties in TPCO crystals are potentially useful for the light amplification, so that TPCO crystals are new class of the powerful candidate for the current injected lasing on organic semiconductors.

Further, recent reports indicate there are a wide variety of optical amplification processes in TPCO systems, such as the stimulated resonance Raman scattering and delayed optical amplification[11, 14, 15]. The stimulated resonance Raman scattering and delayed optical amplification are useful for the wavelength conversion and photonic buffer memory, respectively. In order to realize these applications, we need to produce the optical circuit composed by TPCO films. In this point of view, we have fabricated micro resonator of TPCO films on Si/SiO_2 substrates. Here, we report the results of laser emission in TPCO microcavities. As a result, the fabrication of the microdisks and microrings are effective for the reduction of lasing threshold, so that it will be applicable to organic semiconductor laser fabrications.

Figure 1 shows the flow diagram of the fabrication processes. At first, we used electron beam (EB) lithography to make patterns of microdisks and microrings on the resist. Microdisk and microring patterns were formed on Si substrates by means of reactive ion etching (RIE) with the SF_6 gas. Remained PMMA resist was removed by the RIE with O_2 gas and ultrasonic cleaning in acetone. One of the TPCO, 2,5-bis(4-biphenylyl)thiophene (BP1T) co-oligomer[1,2] films were formed on Si substrates by means of thermal vapor deposition with 400nm thickness. The overcoat layer of amorphous fluorocarbon polymer, Cytop CTX804.5A (ASAHI GLASS Co. LTD. Japan) was spin-coated on a BP1T film with 300nm thickness. The overcoat layer acts as preventing the

evaporation of BP1T molecules during the annealing. The films were annealed on a hot plate and crystallized at 220 °C. The microscope images are shown in the bottom part of Fig. 1. Especially, we can obtain microring cavities with the width of 0.8 μm active region, as shown in the right part of Fig. 1. Hereafter, we indicate the microring cavitiy as the 8-0.8 μm ring cavity. The narrow active region is effective for mode selection of WGM[16]. Both the mode selection and optical confinement in the narrow active region can contribute to reduce the threshold.

We carried out experiments of pulse excitation at 397 nm with a 10-15 ps width onto BP1T microcavities. The spot size was about 100 μm in a diameter. All experiments were carried out at room temperature. Figure 2 shows the laser emission spectra of BP1T microcavities. The excitation density is shown in the unit of μJcm^{-2}. Lasing peaks observed around 2.68-2.70 eV are the 0-1 vibration lines[17]. The lasing spectra show the regular intervals, indicating the whispering gallery modes (WGM) in microdisks and microrings. Mode intervals of all the microcavities are plotted in Fig. 3, as a function of the resonator length L, which is assumed to be the circumference length. The energy intervals are inversely proportional to the circumference length, so that the lasing mode intervals are ascribed to WGM.

Figure 4 shows emission intensity as a function of the excitation density observed in microcavities and bulk film. The lasing threshold values on the microcavities are reduced to 1/2 to 1/5 of that of the bulk film. Especially, we can obtain the minimum threshold on the 8-0.8 μm ring cavity. This is due to the WGM confinement in the narrow waveguide. We also confirmed by using finite deferential time domain (FDTD) calculation that the quality factor, Q, value of the 8-0.8 μm ring cavity was higher by several tens of percent than that of the microdisk cavity. In the calculation, we used the refraction index of 1.8 for BP1T films, which was estimated from the reflection spectrum. Microrings with narrower waveguide are better for further optical confinement in the calculation, but we could not obtained them probably due to the grain boundaries of poly crystalline films.

From the line width of lasing spectra, we obtained the Q of 2000~3000, as shown in Fig. 2. We also estimated the Q value from the lasing threshold. At the lasing threshold of carrier density N_0, the Q value is estimated to be $2\pi n/\sigma N_0 \lambda \sim 1000$. Here, n, σ, and λ are the refractive index, the amplified cross-section and lasing wavelength, respectively. We experimentally estimated N_0 and σ to be 2.5×10^{18} cm^{-3} and 1.0×10^{-16} cm^2 by using the variable stripe length method, respectively. Both the estimated Q values are kept in the same order.

Here, we will estimate the Q value of the actual microcavities. The total Q value is expressed as[18)]

$$Q^{-1} = Q_{abs}^{-1} + Q_{scat}^{-1} + Q_{cav}^{-1}, \qquad (1)$$

$$Q_{scat}^{-1} = Q_{film}^{-1} + Q_{side}^{-1},$$

where Q_{abs}, Q_{scat} and Q_{cav} are determined by the absorption loss, the scattering loss and the cavity finesse. The value Q_{scat} consists of two component. One is Q_{film} which is determined by the scattering loss from film itself such as surface roughness, grain boundaries and cracks of poly crystals, so on. Another is Q_{side} which is determined by the roughness of the side wall in the microcavity. Actually, the quality factor of WGM on the microdisk is strongly dependent on the boundary roughness[19)]. We think roughness and grain boundaries on the side wall limit the quality factor of TPCO microdisks and microrings.

To confirm this, we experimentally estimated the absorption and scattering losses. We measured the emission intensities from the edge of the film without the microcavity. From the measurement, we can estimate both the absorption loss and scattering loss of the film[20)]. The high energy side loss was larger than that of the low energy side. The estimated sum of absorption and scattering losses of BP1T films were concluded to be 0.5 to 30 cm^{-1} from the results, corresponding to the quality factor $Q_{abs}^{-1}+Q_{film}^{-1} \sim 2\pi n/\alpha(=0.5cm^{-1})\lambda \sim 5 \times 10^5$ to 1×10^4.

Q_{cav} was estimated by using 3D-FDTD calculation with three layers. The BP1T film was sandwiched by the SiO_2 layer with the refractive index of 1.46 and the Cytop overcoat film with the

refractive index of 1.34. The side wall of BP1T disks and rings was surrounded by SiO_2. Q_{cav} increased with the increase of the disk diameter. The minimum value of the Q_{cav} in the calculation was estimated to be over 5000 on the disk cavity with the diameter of 8 μm. Q_{cav} on the disk cavity over 10 μm diameter was estimated to be over $1x10^4$.

The estimated values of Q in Eq. (1) are much larger than that of experimental values, except for Q_{side}. Therefore, the Q value of BP1T microcavities are limited by the side wall roughness. In the embedded type of microcavities reported here, the side wall roughness of the SiO_2 layer are considered to be sufficiently small. The grain boundaries and cracks of the poly crystalline film on the circumferential interface are thought to limit the quality factor, and lasing threshold. We need to improve the film quality for further reduction of the lasing threshold.

In the calculation, Q_{cav} increased with the increase of the disk diameter. Contrary, the observed results of the lasing threshold are increasing with the increase of the diameter. Further, on the 8-0.8 μm ring cavity, the threshold is the minimum value. WGM with waveguide confinement is supposed to contribute to the decrease of the threshold.

In summary, we observed the laser emission with WGM on BP1T microdisks and microrings. The lasing threshold is reduced to 1/2 to 1/5 on the microcavities in comparison with the bulk film part. The quality factor of the microcavities are estimated experimentally to be a few thousands. The grain boundaries and cracks of the poly crystalline film on the circumferential interface are thought to limit the quality factor, and lasing threshold. On the microring cavity with the 800nm width of the waveguide, the reduction of the threshold is the maximum. This is supposed to be the WGM confinement in the narrow waveguide.

Reference

1) S. Hotta, H. Kimura, S. A. Lee, and T. Tamaki: J. Heterocyclic Chem. 37, 281 (2000).

2) S. Hotta and M. Goto: Adv. Mater. **14**, 498(2002).

3) M. Ichikawa, H. Yanagi,Y. Shimizu, S. Hotta, N. Suhanuma, T. Koyama and Y. Taniguchi: Adv. Mater. **14**, 1272(2002).

4) K. Nakamura, M. Ichikawa, R. Fushiki, T. Kamikawa, M. Inoue, T. Koyama and Y. Taniguchi, Jpn. J. Appl. Phys. **44**, L1367(2005).

5) H. Yanagi, T. Morikawa and S. Hotta: Appl. Phys. Lett. **81**, 1512(2002).

6) M. Ichikawa, K. Nakamura, M. Inoue, H. Mishima, T. Haritani, R. Hibino, T. Koyama and Y. Taniguchi, Appl. Phys. Lett. **87**, 221113(2005).

7) R. Hibino, M. Nagawa, S. Hotta, M. Ichikawa, T. Koyama and Y. Taniguchi: Adv. Mater. **14**, 119(2002).

8) M. Nagawa, R. Hibino, S. Hotta, H. Yanagi, M. Ichikawa, T. Koyama and Y. Taniguchi: Appl. Phys. Lett. **80**, (2002)544.

9)M. Ichikawa, R. Hibino, M. Inoue, T. Haritani, S. Hotta, K. Araki, T. Koyama, and Y. Taniguchi, Adv. Mater. **17**, 2073 (2005).

10) K. Shimizu, Y. Mori, and S. Hotta, J. Appl. Phys. **99**, 063505 (2006).

11) H. Yanagi, A. Yoshiki, S. Hotta and S. Kobayashi: Appl. Phys. Lett. **83**, (2003)1941.

12) K. Shimizu, D. Hoshino and S. Hotta: Appl. Phys. Lett. **83**, (2003)4494.

13) S. Kobayashi, F. Sasaki, H. Yanagi, S. Hotta, M. Ichikawa and T. Taniguchi: J. Lumin. **112**, (2003)325.

14) H. Yanagi, A. Yoshiki, S. Hotta and S. Kobayashi: J. Appl. Phys. **96**, (2004)4240.

15) F. Sasaki, S. Kobayashi, S. Haraichi, H. Yanagi, S. Hotta, M. Ichikawa and Y. Taniguchi, Jpn. J. Appl. Phys. **45**(2006)L1206.

16) M. Kuwata-Gonokami and K. Takeda, Opt. Mater. **9**(1998)12.

17) K. Bando, T. Nakamura, Y. Masumoto, F. Sasaki, S. Kobayashi and S. Hotta: J. Appl. Phys. **99**, (2006)013518.

18) S. V. Frolov, M. Shkunov, Z. V. Vardeny and K. Yoshino: Phys. Rev. B**56**, (1997)R4363.

19) A. I. Rahachou and I. V. Zozoulenko, J. Appl. Phys. **94**, (2003)7929.

20) M. D. McGehee, R. Gupta, S. Veenstra, E. K. Miller, M. A. Diaz-Garcia, A. J. Heeger, Phys. Rev. B**58**, 7035(1998).

Figure Caption

Fig. 1. The upper part shows schematic drawing of fabrication processes of microcavities; (a) EB lithography, (b) SF_6-RIE of Si substrates, (c) O_2-RIE of the remained PMMA film, (d) SiO_2 sputtering, and (e) thermal deposition of BP1T films and overcoating of cytop films. The middle part shows the molecular structure of BP1T co-oligomer. The bottom part shows the microscope image of 10 μm and 20μm disks and 8 μm rings with the 800 nm width.

Fig. 2. Lasing spectra of BP1T microcavities. The disk and ring diameter and excitation density are shown in the figure.

Fig. 3. Mode intervals ΔE observed on microcavities.

Fig. 4. Excitation density dependence of spectral peaks of the 0-1 line on the microring and microdisks. Results on all microcavities show clear lasing threshold.

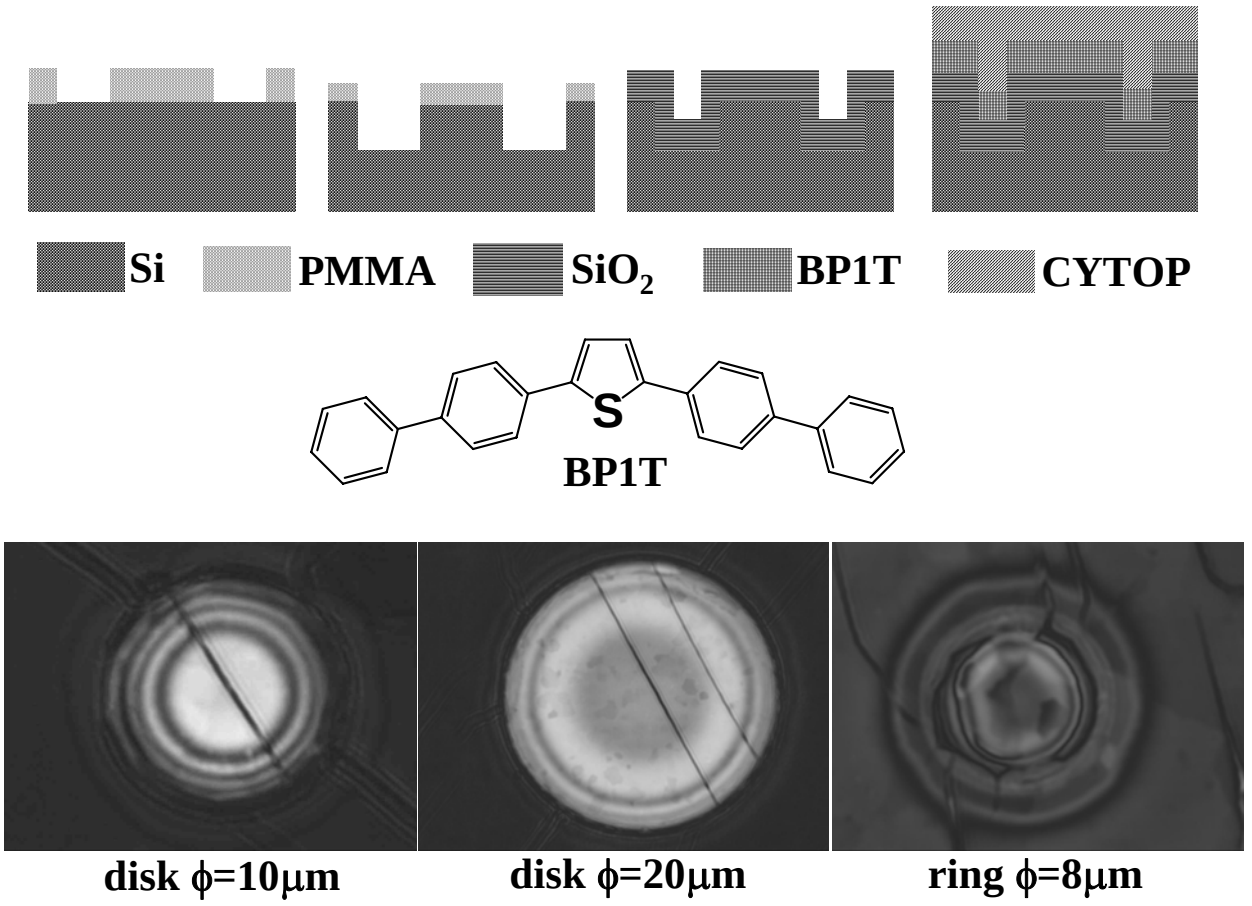

Fig. 1. The upper part shows schematic drawing of fabrication processes of microcavities; (1) EB lithography, (2) RIE of Si substrates, (3) SiO_2 sputtering, and (4) thermal deposition of BP1T films and overcoating of cytop films. The middle part shows the molecular structure of BP1T co-oligomer. The bottom part shows the microscope image of 10 μm and 20μm disks and 8 μm rings with the 800 nm width.

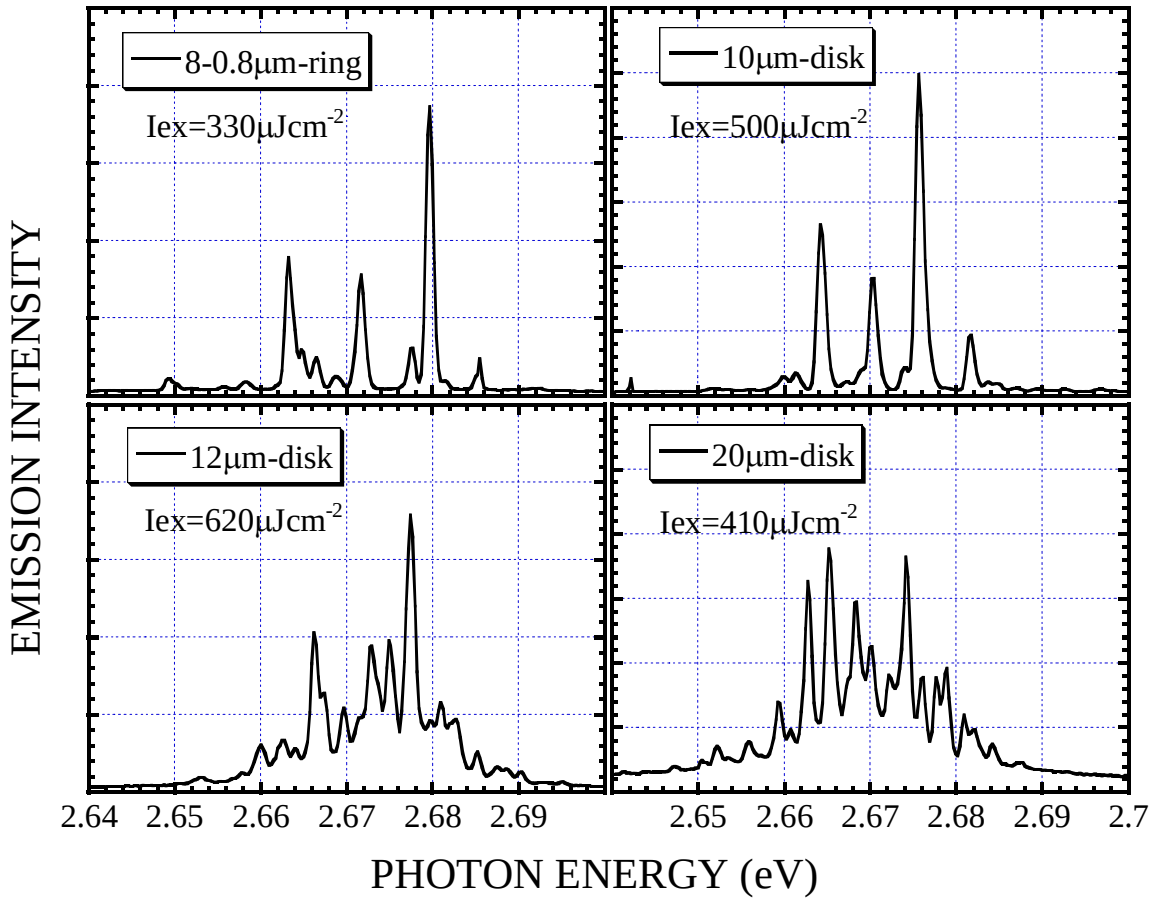

Fig. 2. Lasing spectra of BP1T microcavities. The disk and ring diameter and excitation density are shown in the figure.

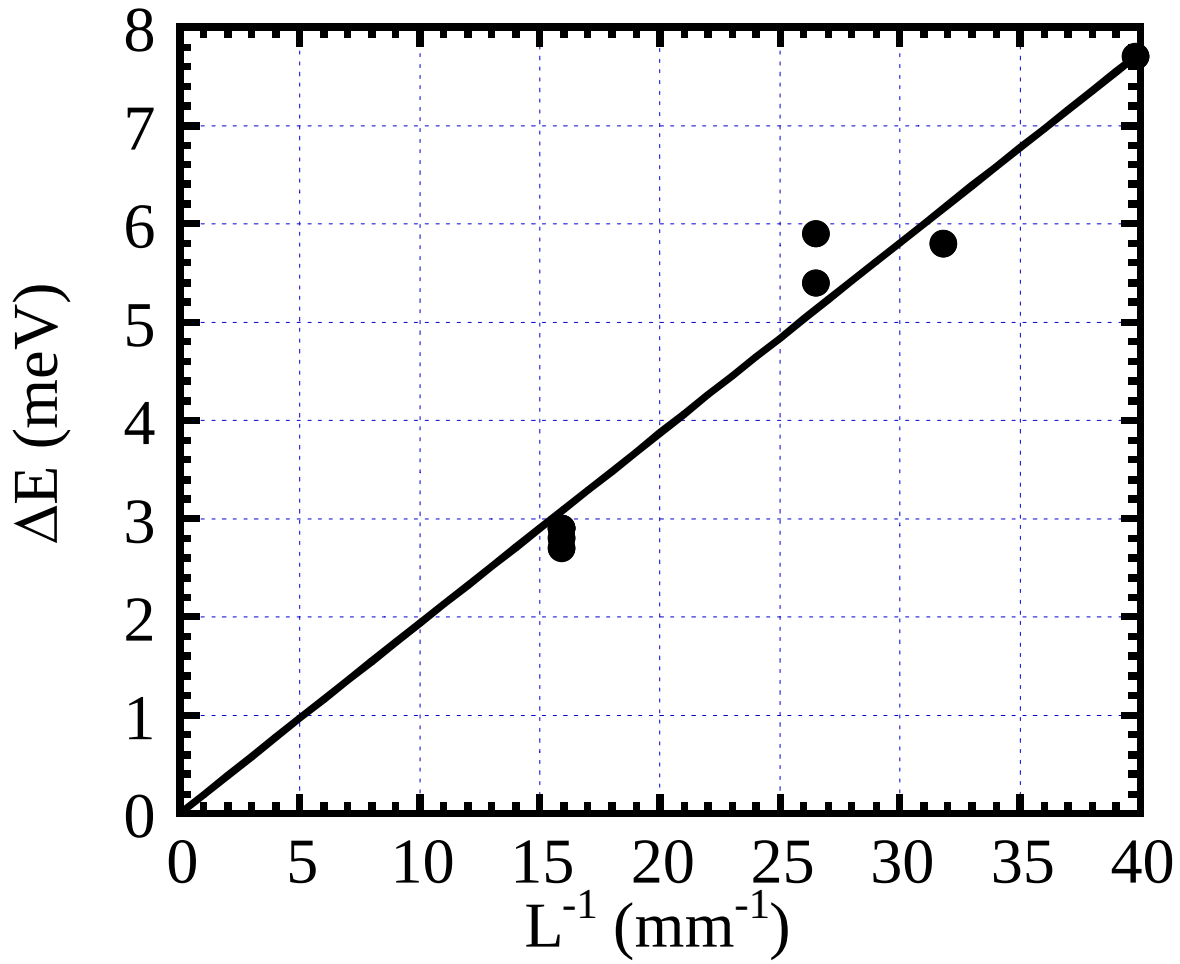

Fig. 3. Mode intervals ΔE observed on microcavities.

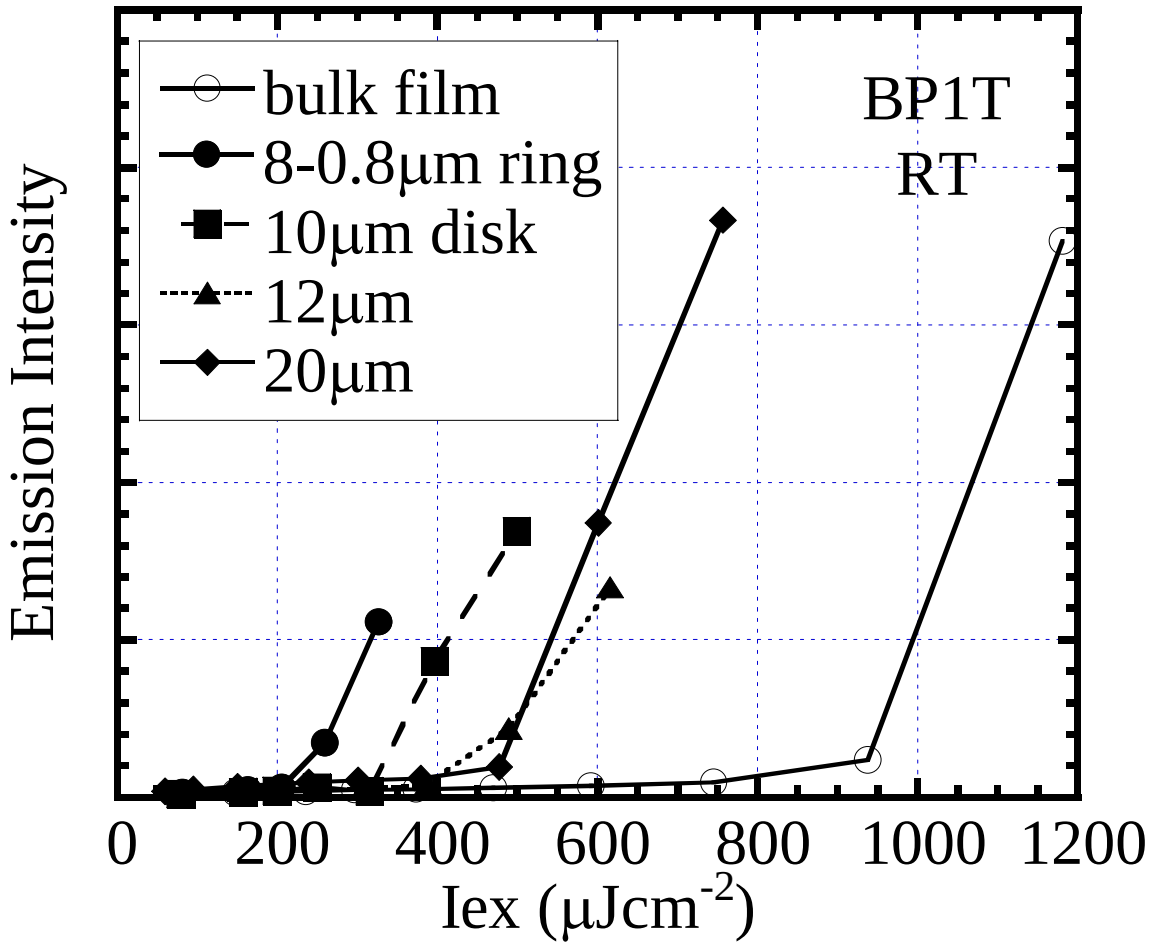

Fig. 4. Excitation density dependence of spectral peaks of the 0-1 line on the microring and microdisks. Results on all microcavities show clear lasing threshold.